Overall Stability Analysis of Anchored Sheet Pile Structures

A.H. SOUBRA & P. REGENASS
ENSAIS, 24, Bd de la Victoire, 67084 Strasbourg Cedex, France

ABSTRACT
The overall stability analysis of anchored sheet pile structure is investigated by a theoretical model using the upper-bound method of the limit analysis theory. A translational failure mechanism is considered for the calculation scheme. This mechanism is composed of two rigid blocks in the active zone and the so-called log-sandwich mechanism in the passive zone. The numerical results show good agreement with experimental results obtained from laboratory model tests.

INTRODUCTION

Early anchored sheet pile structures comprised a sheet pile wall, an anchor rod and an anchor wall or plate parallel to the sheet pile wall. In the past, the necessary length of the rod was determined by searching not intersecting slip surfaces of the active wedge behind the retaining wall and the passive wedge in front of the anchor plate.

Since the preceding design procedure proved not to be adequate, Kranz (1940) proposed a method that took into account a failure surface that extends from the base of the retaining wall to the base of the anchor plate. This method has been extended to cement grout injection anchors and pile tie-backs even though the load transfer is completely different. In this paper a modified approach of the Kranz method is proposed where the failure of the whole soil in front and behind the retaining structure is taken into consideration.

The approach presented in this paper is based on the upper-bound theorem of the limit analysis theory. The solution so obtained is a rigorous upper-bound solution to the exact solution for an associated flow rule Coulomb material obeying Hill's maximal work principle.

THEORETICAL ANALYSIS

As it is well known, the upper-bound theorem states that the soil mass will collapse if there is any compatible pattern of plastic deformation for which the rate of work of the external loads exceeds the part of internal dissipation. Thus, for a kinematically admissible velocity field, an upper bound of the exact solution can be obtained by equating the power dissipated internally to the power expended by the external loads. A kinematically admissible velocity field is one that satisfies the flow rule, the velocity boundary conditions, and compatibility. During plastic flow, power is assumed to be dissipated by plastic yielding of the soil mass, as well as by sliding along velocity discontinuities where jumps in the normal and tangential velocities may occur.

Ground anchorages and anchored structures. Thomas Telford, London, 1997.

Note that the velocity field at collapse is often modelled by a mechanism of rigid blocks that move with constant velocities. Since no general plastic deformation of the soil mass is permitted to occur, the power is dissipated solely at the interfaces between adjacent blocks, which constitute velocity discontinuities. This kind of velocity field will be used herein. Finally, note that the analysis of the overall stability of an anchored sheet pile structure by the upper-bound theorem gives an unsafe estimate of the safety factor.

In this paper, a translational failure mechanism is considered for the calculation of the safety factor. This mechanism is based on the experimental observations on laboratory model tests with Shneebeli rollers (Masrouri 1986, Masrouri & Kastner 1991) and it will be presented in some details in the following sections.

Hypotheses

The following assumptions have been made in the analysis:

- The soil is homogeneous and isotropic. It is an associated flow rule Coulomb material obeying Hill's maximal work principle. It is characterised by its angle of internal friction ϕ and its cohesion c.
- The friction at the soil-wall interface is characterised by a constant angle of friction δ $(\delta \leq \phi)$. This is in conformity with the kinematics proposed in this paper.
- The sheet pile wall and the anchor are assumed to be rigid.
- No pore water pressures are considered in the present analysis.
- The overall stability analysis of the anchored sheet pile is investigated as a two-dimensional plane strain problem.
- The safety factor considered in the present analysis is defined as the ratio of the resisting work to the work of the driving external forces.

Failure Mechanism

As it has been shown by Masrouri (1986), the sheet pile wall moves horizontally. Hence, the soil behind the sheet pile will be in an active state and the soil in front of the wall will be in a passive state. The stereophotogrammetric image of failure given by Masrouri has shown that there are three different zones around the sheet pile wall: i) Two zones in the active state behind the wall, ii) one zone in the passive state in front of the wall. Hence, the failure mechanism adopted in this paper (cf. figure 1) consists of:

- A triangular active wedge EFG. This block is rigid and it is completely described by two angular parameters θ_1 and θ_2.
- A quadrilateral rigid block GFAD. This block passes through the toe of the sheet pile wall.
- A zone CDHIJ in front of the sheet pile wall. This zone is in a passive state. The failure mechanism considered in this zone is a log-sandwich. It is composed of a radial shear zone CHI bounded by a log-spiral curve of angle ϕ. This radial shear zone is sandwiched between two triangular rigid blocks CDH and CIJ. The log sandwich mechanism is completely defined by two angular parameters θ_3 and θ_4. The choice of this failure mechanism in the passive zone is not arbitrary. Chen (1975) have considered six translational mechanisms to calculate the passive earth pressures. The numerical results obtained have shown that the log sandwich is the best mechanism since it gives the smallest upper-bound solutions in most cases.

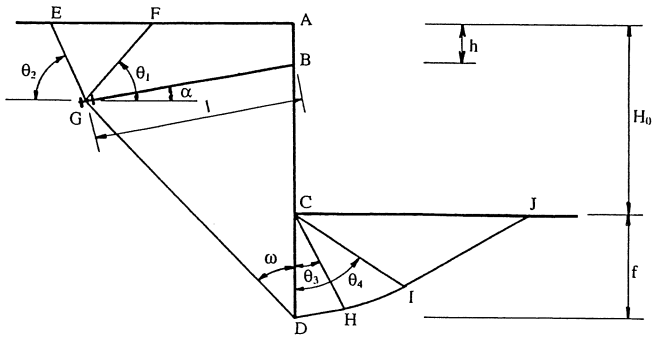

Figure 1 : Theoretical failure mechanism

Kinematics of the Failure Mechanism

As it has been mentioned before, the upper-bound method in limit analysis requires a kinematically admissible failure mechanism which satisfies the velocity boundary conditions. In the case of a Coulomb (ϕ, c) material, the velocity along a velocity discontinuity must be inclined at an angle ϕ with this surface. For the present analysis, this condition is satisfied on all the velocity discontinuities except along the sheet pile wall, where we have made the assumption of sliding by friction (cf. figure 2). Thus, the velocities along the sheet pile wall are assumed tangent to this wall. In the active zone, the blocks EFG and GFAD move as rigid bodies with velocities V_1 and V_2 respectively. The sheet pile wall moves horizontally with velocity V_p. On the other hand, the velocity field in the passive zone consists of the two triangular rigid blocks CDH and CIJ which move with velocities V_3 and V_4 respectively. This zone includes also the radial shear zone bounded by the log spiral slip surface HI. The velocity field in the shear zone is of the translational type and the velocity distribution along the surface HI is given by the following relationship (cf. Chen 1975):

$$V(\theta) = V_3 \exp\left[(\theta - \theta_3)\tan\phi\right] \qquad (1)$$

The velocity hodographs of the active and the passive zones are shown in figure (3). The velocity field is now completely defined. The work equation of the upper-bound theorem in limit analysis is given in the following section.

Work Equation of the Failure Mechanism

The work equation consists in equating the rate of external work done by the external forces to the rate of internal energy dissipation along the plastically deformed surfaces.

The incremental external work due to an external force is the external force multiplied by the corresponding incremental displacement or velocity. The external forces contributing in the external work consist of the weight of the different blocks EFG, GFAD, CDH, CHI and CIJ. The incremental external work due to self weight in a region is the vertical component of the velocity in that region multiplied by the weight of the region. The incremental external work for the different external forces can be easily obtained. They are not presented herein.

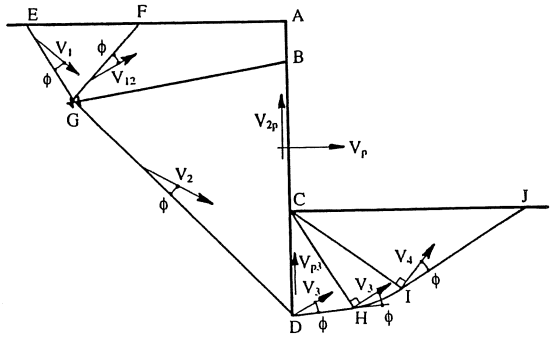

Figure 2 : Velocity field

The incremental energy dissipation per length unit along a velocity discontinuity or a narrow transition zone can be expressed as follows:

$$\Delta D_L = c.\Delta V.\cos\phi \qquad (2)$$

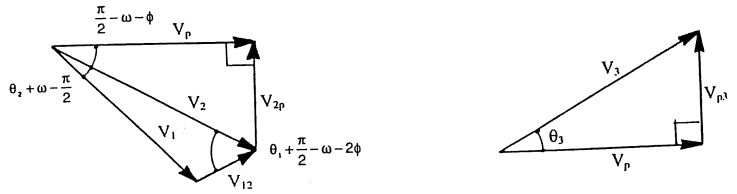

Figure 3 : Velocity hodograph a) in the active zone b) in the passive zone

where ΔV is the incremental displacement or velocity which makes an angle ϕ with the velocity discontinuity according to the associated flow rule of perfect plasticity, and c is the cohesion parameter. The incremental energy dissipation along the different velocity discontinuities EG, GF, GD, DH, HI, IJ and $r_i(\theta)$ can be easily calculated. They are not presented herein. Finally, it is to be noted that along the soil-structure interface where we have adopted the assumption of sliding by friction, the energy dissipation is given as follows:

$$\Delta D_L = P.\tan\delta.V \qquad (3)$$

where P is the normal force acting on the discontinuity surface and V is the tangential velocity along this surface.

Along the sheet pile wall, the energy dissipation is given by:

$$\Delta D_L = P_1 . \tan\delta . V_{2p} + P_2 . \tan\delta . V_{p3} \quad (4)$$

where P_1 and P_2 are the normal forces acting on the surfaces AD and CD respectively. These forces (i.e. P_1 and P_2) are determined by considering the work equation in both the active and the passive zones separately.

CALCULATION PROCEDURE

The different steps of the calculation procedure are as follows:

- One considers separately the active and the passive zones and considers the work equation for each zone in order to determine the forces P_1 and P_2 for given values of the angular parameters θ_1, θ_2, θ_3 and θ_4.
- One calculates the different terms of the work equation contributing in the energy dissipation and the ones contributing in the positive external work due to the driving forces.
- One then calculates the safety factor defined above as the ratio of the energy dissipation to the positive external work for given angular parameters θ_1, θ_2, θ_3 and θ_4.
- Finally, one minimises the safety factor with respect to the four angular parameters to obtain the minimal safety factor and the corresponding critical failure mechanism.

NUMERICAL RESULTS

In this section, we will present the numerical results showing the influence of the different parameters of the anchored sheet pile (i.e. the excavation level, the anchor's length and inclination) on the safety factor and the corresponding critical failure mechanism. This study is accompanied by a comparison of the present results with those obtained from the laboratory model tests with Shneebeli rollers (Masrouri 1986). The data which concern the laboratory model are as follows: H_0+f=80.5cm ; h=5cm ; ϕ=21° ; δ=8° ; γ=65kN/m^3 (cf. figure 1 for the notations).

Influence of the Excavation Level

Figure (4) shows the variation of the safety factor F_s with H_0 where H_0 represents the distance between the excavation level and the top of the sheet pile. It is clear that F_s decreases with H_0. To show the influence of the excavation level on the critical failure surface, one presents in figure (5) the critical surfaces for two values of H_0 (H_0=40cm and 53cm).

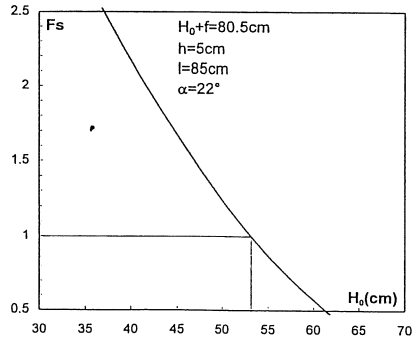

Figure 4 : Variation of the safety factor F_s with the excavation depth H_0

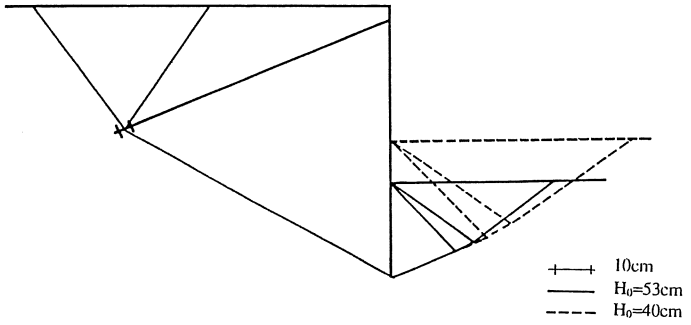

Figure 5 : Influence of the excavation level on the critical failure surface

For the case H_0=40cm, there is stability (F_s=2.18). However, the minimal excavation level for which the failure occurs (F_s=1) corresponds to H_0=53cm. It is to be noted that the critical failure surface in the active zone is independent of the excavation level. The angular parameters θ_1 and θ_2 obtained from the numerical minimisation are both equal to $\pi/4+\phi/2$. On the other hand, the angles $I\hat{C}J$ and $I\hat{J}C$ are both equal to $\pi/4-\phi/2$ and the wedge CIJ is in a Rankine limit equilibrium state.

Influence of the Anchor Length

Figure (6) shows the variation of the safety factor F_s with the anchor length l when H_0=50.5cm and α=22°. This factor increases with the anchor length increase. Notice however that due to economical and practical reasons, very long anchors are not used in geotechnical engineering.

To show the influence of the anchor length on the critical failure surface, we present in figure (7) the two failure surfaces corresponding to two values of the anchor length (l=75cm and 100cm). It is obvious that for l=100cm, there is stability (F_s=2.07). However, the minimal anchor length for which the failure occurs (F_s=1) corresponds to l=75cm.

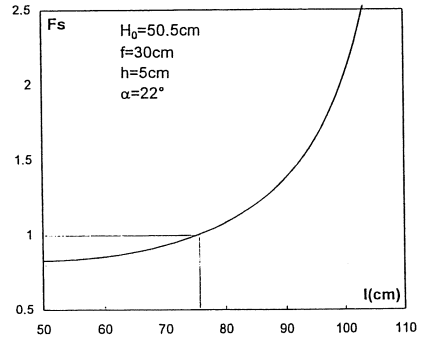

Figure 6 : Variation of the safety factor F_s with the anchor length l

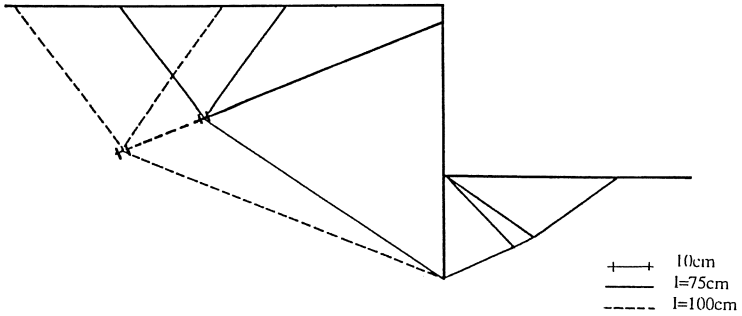

Figure 7 : Influence of the anchor length l on the critical failure surface

It is obvious that the angles θ_1 and θ_2 obtained from the numerical minimisation are both equal to $\pi/4+\phi/2$ independently of the anchor length. On the other hand, the wedge CIJ in the passive zone is in a Rankine limit equilibrium state.

Influence of the Anchor Inclination

Figure (8) shows the variation of the safety factor F_s with the anchor inclination α when H_0=49cm and l=75cm. This factor increases with the anchor inclination increase. Notice however that the practical engineer is limited by a maximal value of α for practical purposes.

To show the influence of the anchor inclination on the critical failure surface, we present in figure (9) the two failure surfaces corresponding to two values of the anchor inclination (α=12° and 35°). The failure case (F_s=1) occurs for α=12°. However, for α=35°, F_s=1.25. Finally, it is to be noted here that the same conclusions mentioned above and concerning the evolution of the angular parameters, are also valid in the present case.

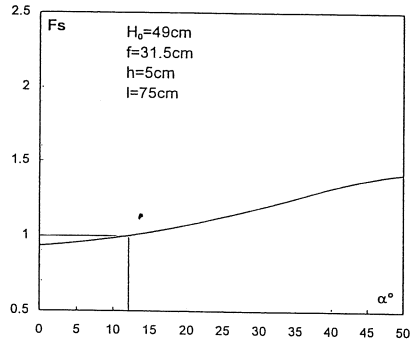

Figure 8 : Variation of the safety factor F_s with the anchor inclination α

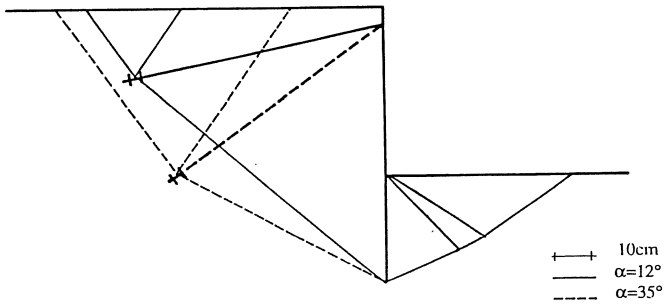

Figure 9 : Influence of the anchor inclination on the critical failure surface

Comparison with the Experimental Data

Table (1) presents the values of the excavation depth H_0 corresponding to the limit state (Fs=1) obtained from the laboratory model tests with Schneebeli rollers (Masrouri 1986) and those obtained from the present theoretical model.

Anchor lenght l(cm)	Anchor inclination α°	Critical excavation depth H_0 (cm)		Percent difference
		Masrouri (1986)	Present solution	
85	22	50.5	53	4.9
75	22	49	50	2
65	22	47	48	2.1
55	22	42.5	47	10
55	31	45	47.5	5.5
75	31	51	52	2

Table 1 : Critical values of the excavation depth H_0 corresponding to failure (F_s=1)

It is obvious that there is good agreement between the experimental and the theoretical values.

CONCLUSIONS

The theoretical analysis of the overall stability of an anchored sheet pile wall has shown that the stability increases with the anchor's length and inclination and that the excavation depth corresponding to overall failure (F_s=1) of the soil-structure system is in good agreement with the experimental observations on laboratory model tests.

REFERENCES

Heibaum, M. (1993). Overall stability of anchored retaining walls. International Symposium on Limit State Design in Geotechnical Engineering, ISLSD, Copenhagen, Vol 2, Danish Geotechnical Society, pp 331-340.

Kastner, R. (1982). Excavations profondes en site urbain: problèmes liés à la mise hors d'eau. Dimensionnement des soutènements butonnés. Thèse de Docteur ès Sciences, INSA Lyon et Université Claude Bernard, Lyon I, 409p.

Kranz, E. (1940). Uber die Verankerung von Spundwanden. Mitteilungen aus dem Gebiete des Wasserbaus und der Baugrundforschung, Heft 11. Berlin: Ernst & Sohn.

Masrouri, F. (1986). Comportement des rideaux de soutènement semi-flexibles : étude théorique et expérimentale. Thèse de Doctorat, INSA Lyon, 247p.
Masrouri, F, & Kastner, R. (1991). Essais sur modèle de rideaux de soutènement ; confrontation à diverses méthodes de calcul. Revue Française de Géotechnique, N° 55, pp 17-33.

Limit Loads of Strip Anchors

P. REGENASS & A.H. SOUBRA
ENSAIS, 24, Bd de la Victoire, 67084 Strasbourg Cedex, France

ABSTRACT
The limit loads of strip anchor plate are calculated using the upper-bound method of the limit analysis theory. Several translational failure mechanisms are considered for the calculation schemes. The numerical results obtained are presented and compared with other authors results.

INTRODUCTION

Anchors are structural elements used in civil engineering practice and designed primarily to resist pullout (tensile) loads. They are used extensively for structures subjected to overturning moments or pullout forces. Electrical transmission towers and retaining walls are typical examples for such structures. Anchors are manufactured in a variety of configurations such as anchor plates, pile anchors, grouted anchors, prestressed concrete anchors, and single-and multiple screw helical anchors. This paper is concerned with the limit loads of anchor plate subjected to axial uplift forces.

Depending upon the depth of embedment of the plate in the soil, the anchor is classified as : i) Shallow anchor; or ii) deep anchor. In the former, the anchor is installed close to the surface of the soil, and the failure surface in the soil extends from the tip of the anchor to the ground surface with significant surface movements. A slight increase in depth results in a considerable increase in the breakout load. However, for the deep anchor condition, the failure surface in soil at ultimate load does not extend to the ground surface (i.e. local shear failure in soil located around the anchor takes place). Most authors assume that the shallow anchor condition exists for $H/h \leq 5$. In this paper, only the shallow anchor condition will be considered in the analysis.

A literature survey indicates that numerous methods have been proposed by many investigators to design anchors subjected to uplift uniaxial forces (Ovesen & Stroman, 1972; Neely, Stuart & Graham, 1973; Das & Seely, 1975; Rowe & Davis, 1982; Dickin & Leung, 1983; Vermeer & Sutjiadi, 1985; Murray & Geddes, 1987). Most of these have dealt with horizontal or/and vertical anchors and have been based on the results of tests on small-scale models in the laboratory, which may be subject to considerable scale effects.

The previous theoretical research into anchor behaviour has focused on elastic response (Fox, 1948; Douglas & Davis, 1964; Rowe & Booker, 1979) and ultimate capacity. Many investigators have proposed approximate techniques for determining the collapse load of anchor plates. Approaches involve the use of either limit equilibrium concepts or the method

Ground anchorages and anchored structures. Thomas Telford, London, 1997.